ELSEVIER

Journal of Nuclear Materials 276 (2000) 65–77

journal of nuclear materials

www.elsevier.nl/locate/jnucmat

# Stability and mobility of defect clusters and dislocation loops in metals

Yu.N. Osetsky[a,*], D.J. Bacon[a], A. Serra[b], B.N. Singh[c], S.I. Golubov[c]

[a] *Department of Materials Science and Engineering, The University of Liverpool, Brownlow Hill, Liverpool L69 3GH, UK*
[b] *Dept. Matematica Aplicada III, Universitat Politecnica de Catalunya, Jordi Girona 1-3, E-08034 Barcelona, Spain*
[c] *Materials Research Department, Risø National Laboratory, DK-4000 Roskilde, Denmark*

**Abstract**

According to the production bias model, glissile defect clusters and small dislocation loops play an important role in the microstructural evolution during irradiation under cascade damage conditions. The atomic scale computer simulations carried out in recent years have clarified many questions about the structure and properties of glissile clusters of self-interstitial atoms that are formed directly in the cascade volume. It has been found that such clusters consist of sets of crowdions and are highly mobile in the crowdion direction. Very recently, one-dimensional glide of similar character has been observed in the computer simulation of small vacancy loops in α-Fe. In the present paper we summarise results obtained by molecular dynamics simulations of defect clusters and small dislocation loops in α-Fe(bcc) and Cu(fcc). The structure and stability of vacancy and interstitial loops are reviewed, and the dynamics of glissile clusters assessed. The relevance and importance of these results in establishing a better understanding of the observed differences in the damage accumulation behaviour between bcc and fcc metals irradiated under cascade damage conditions are pointed out. 

## 1. Introduction

Within the last decade a large number of molecular dynamics (MD) simulation studies have been made of displacement cascades generated by energetic recoils in metals (see reviews [1–5]). Most simulations have been carried out on fcc copper [5–7] and bcc iron [8–11]. One of the most important findings of these studies is that clusters of self-interstitial atoms (SIAs) form within the cascade volume during the cooling down phase of cascades. MD simulations have also established the significant fact that a large portion of these SIA clusters are small, glissile dislocation loops and highly mobile in one direction. It is interesting to note that indirect experimental evidence for intracascade clustering and one-dimensional glide of SIA clusters has existed in the literature for some time (see [12,13]).

The emergence of these features of defect production in displacement cascades, and the fact that SIA clusters are thermally more stable than vacancy clusters, imply that the problem of defect accumulation under cascade-damage conditions cannot be treated within the framework of the standard rate theory which does not take into account the one-dimensional transport of clusters. The recognition of this led to the concept of production bias [14–16]. The production bias model (PBM) has been developed to include the effect of glissile clusters (produced in cascades) on the kinetics of damage accumulation [12,13,16], and recently consideration of 'size distribution functions' has been incorporated in the calculations of defect accumulation within the framework of the PBM [17]. This refinement makes the calculation of defect accumulation more quantitative and allows explicit inclusion of the contribution of sessile-glissile loop transformation (in the presence of vacancy super-saturation). Thus, the PBM in the present form [17,18] provides a theoretical framework within which the accumulation of defects in the form of defect clusters (dislocation loops, stacking fault tetrahedra (SFT)) and voids can be calculated. It should be recognized,

* Corresponding author. Tel.: +44-151 794 5384; fax: +44-151 794 4675.
*E-mail address:* osetsky@liverpool.ac.uk (Yu.N. Osetsky)

0022-3115/00/$ - see front matter 
PII: S0022-3115(99)00170-1

however, that the accuracy of the results is limited by the accuracy of the information available on the main damage parameters, i.e., fractions of glissile and sessile clusters of SIAs, and the properties, i.e., stability and mobility, of the clusters produced in the cascades. MD simulations of cascades yield information on the fractions of clustered and single defects generated in the cascades, but this is not enough for an accurate description of the damage accumulation behaviour because the PBM requires knowledge of the glissile fraction of the SIA clusters and their mobility. This information is not readily available at present and this makes it difficult to rationalize the differences in the observed defect accumulation behaviour between fcc and bcc metals and alloys [19]. An example of such differences is the observed cluster density in copper and α-iron irradiated with fission neutrons, as shown in Fig. 1 [20]. Similar differences in cluster density between self-ion irradiated copper and iron have been reported earlier in [19,21]. The results of MD simulations [4,5], on the other hand, show that the differences in the size and number of SIA clusters (formed in the cascades) between copper and iron are rather small and are inadequate for explaining the large differences observed experimentally (Fig. 1).

As pointed out by Singh and Evans [19], quite possibly it is the ratio of the glissile to sessile fractions of SIA clusters produced in the cascades which causes these large differences in the defect accumulation behaviour between copper and iron. Whether or not the crystal structure itself plays any significant role in determining this ratio and the cluster mobility is not well known. Thus, in order to improve our understanding of the defect accumulation processes under cascade damage conditions it is essential to establish a clear and detailed understanding of the nature and properties of the clusters produced both in cascades and in the bulk. This need led us to initiate investigations to determine the structure and properties of SIA and vacancy clusters in copper and iron using the MD technique. In this paper we present an overview of the results obtained during the last few years [22–28] and also new unpublished results. Attention is focused on the common and specific properties of clusters in Cu and Fe.

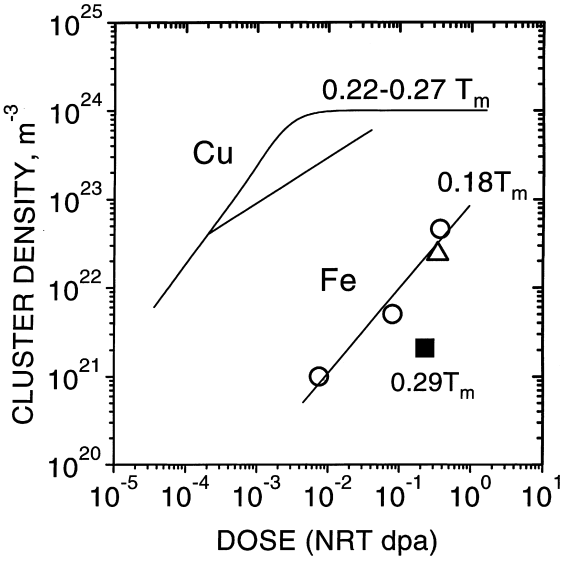


Fig. 1. Dose dependence of cluster density measured in α-iron [20] and Cu [56] irradiated with fission neutrons at temperatures below the recovery stage $V$, i.e., $<0.3T_m$, where $T_m$ is the melting temperature. Note the big difference in the cluster density between iron and copper.

The studies used molecular dynamics and statics simulations. A variety of crystallite shapes, sizes and boundary conditions were used, depending on the particular problem. To study the sensitivity of the results to the form of interatomic interactions, we have used two types of interatomic potential. They are many-body potentials (MBPs) of Finnis–Sinclair type described in [29,30] and long-range pair potentials (LRPPs) obtained in [31] within the pair approximation of the generalized pseudopotential theory [32,33]. Although the potentials reproduce similar sets of properties they are qualitatively different in form. For example, the MBPs are short-range and describe equilibrium crystals whereas the LRPP are long-range and non-equilibrium. This difference affects some properties of defect clusters, but the majority of the results obtained are qualitatively similar. The details of the simulations and comparison of properties of the potentials used can be found in [22,23,31].

## 2. Structure and stability of defect clusters

### 2.1. Interstitial clusters and loops in iron

The structure and stability of SIA clusters and loops in α-Fe have been studied in [23,34]. The structure of small clusters does not depend on either the number of interstitials or the potentials. The results for both potentials have shown that the most stable configuration of all clusters is a set of ⟨1 1 1⟩ crowdions. This is in agreement with recent MD results [8,11,34,35] showing that small stable clusters (containing $N_I = 2$–10 interstitials) are sets of ⟨1 1 1⟩ crowdions in a {1 1 0} plane.

These results differ slightly from earlier studies on Fe [36,37] where static relaxation was applied to initial configurations of ⟨1 1 0⟩ dumbbells. The potentials used reproduce the ⟨1 1 0⟩ dumbbell as the stable SIA and it was concluded that sets of ⟨1 1 0⟩ dumbbells in a {1 1 0} plane are stable for clusters with $N_I \leqslant 4$. The transformation from ⟨1 1 0⟩ dumbbells into a configuration of

⟨1 1 1⟩ crowdions started at $N_I = 5$–7 with rotation of the habit plane. A cluster of 16 interstitials was found to be (1/2) ⟨1 1 1⟩ {1 1 1} edge dislocation loop. We have tested these configurations with the Johnson potential for Fe [38] used in [36] and found that the difference in the stable configurations of small clusters can be explained by differences in the simulation methods used. Thus, in static relaxation a metastable set of more than two ⟨1 1 0⟩ dumbbells can be formed although it is unstable with respect to the ⟨1 1 1⟩ state when annealed using the MD simulation technique.

A qualitatively new result obtained in [23] is that small clusters of ⟨1 0 0⟩ crowdions have relatively high stability. In general, they have a higher stability with the LRPP than with the MBP. Note that ⟨1 0 0⟩ clusters can be obtained after relaxation of initially created sets of ⟨1 1 0⟩ dumbbells.

Among bigger clusters having more than about 7 SIAs only two configurations are stable, namely sets of ⟨1 1 1⟩ or ⟨1 0 0⟩ crowdions, and they may act as nuclei of interstitial dislocation loops with Burgers vectors $\boldsymbol{b}$ equal to (1/2) ⟨1 1 1⟩ or ⟨1 0 0⟩, respectively. As an example, cross-sections through the centre of clusters of 37 ⟨1 1 1⟩ crowdions and 37 ⟨1 0 0⟩ crowdions modelled with the LRPP are presented in Fig. 2(a) and (b), respectively. It can be seen that, although all the individual interstitials can be recognised, both clusters have the structure of dislocation loops. Such clusters/loops having up to 217 SIAs have been studied [23,34] and the results for the binding energy of the most stable (1/2) ⟨1 1 1⟩ and ⟨1 0 0⟩ perfect dislocation loops are presented in Fig. 3 for the LRPP. Loops were studied with different habit planes, and it was found that in the size range studied, pure edge loops ((1/2) ⟨1 1 1⟩ {1 1 1} and ⟨1 0 0⟩ {1 0 0}) are stable but have slightly lower binding energy [24] than non-edge loops. Examples of configurations of such perfect non-edge and edge SIA loops with Burgers vectors (1/2) ⟨1 1 1⟩ and ⟨1 0 0⟩ can be found in [23,27]. In MD simulations at $T > 0$ K a loop of either type changes its habit plane between non-edge and edge configurations continuously.

It should be noted that all stable SIA clusters and loops studied using MD simulations in Fe are found to be intrinsically glissile because of the perfect character of their Burgers vector [23].

### 2.2. Interstitial clusters and loops in copper

For both types of potentials for copper, the ⟨1 0 0⟩ dumbbell is the stable configuration of the SIA and the smallest cluster is stable as two ⟨1 0 0⟩ dumbbells [9,23–25,28]. Bigger clusters can be stabilised in one of two different configurations, however. One is a set of ⟨1 0 0⟩ dumbbells and the other a set of ⟨1 1 0⟩ crowdions, and both may have a {1 1 1} habit plane. During growth, these clusters transform into Frank faulted loops (1/3)

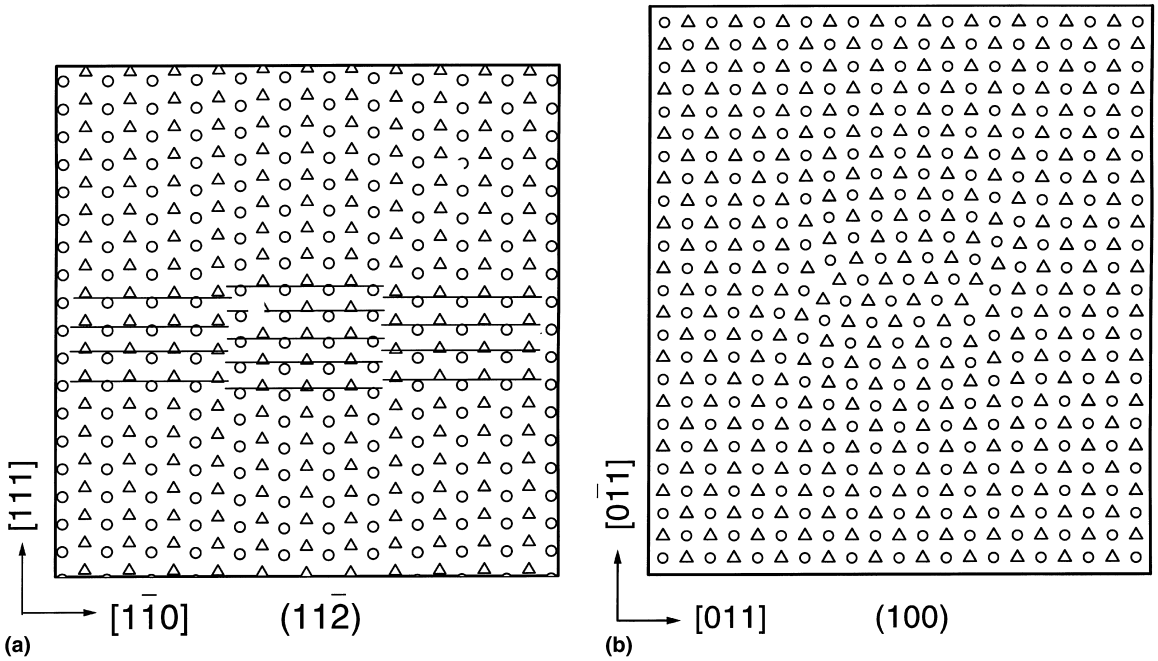


Fig. 2. Cross-sections through the centre of hexagon loops with $N_I = 37$ relaxed with the LRPP: (a) (1 1 $\bar{2}$) cross-section of a loop with $\boldsymbol{b} = (1/2)$ [1 1 1] and (b) (1 0 0) cross-section of a loop with $\boldsymbol{b} = [1\,0\,0]$. Different symbols indicate different atomic planes, and lines are given as a guide for the eye.

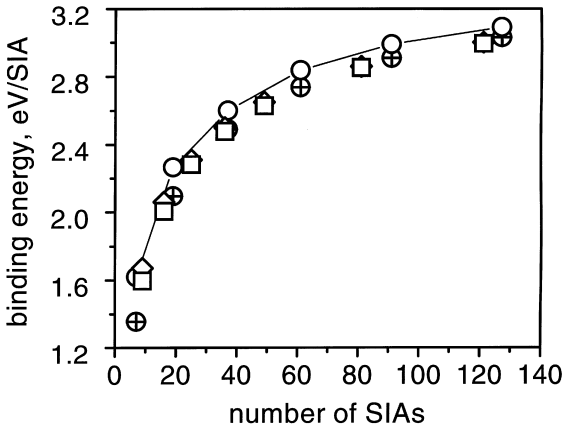


Fig. 3. Binding energy for SIA loops of different shape and Burgers vectors in Fe modelled using the LRPP. Hexagonal loops: open circle: (1/2) ⟨1 1 1⟩ {1 1 1}, crossed circle ⟨1 0 0⟩ {1 0 0}. Square loops: diamond: (1/2) ⟨1 1 1⟩ {1 1 1}, square: ⟨1 0 0⟩ {1 0 0}.

⟨1 1 1⟩ {1 1 1} and perfect loops (1/2) ⟨1 1 0⟩ {1 1 0}, respectively [23]. In general, the stability of both types is similar, with a small preference for ⟨1 1 0⟩ crowdions and perfect loops at big sizes (see Fig. 4). An example of the structure of a Frank loop is presented for $N_I = 37$ in Fig. 5, where the stacking fault in the centre of the loop can be clearly seen. The structure of the perfect (1/2) ⟨1 1 0⟩ {1 1 0} loop depends on its shape as well as size. Thus, small hexagonal (or circular) loops have edge perfect structure as shown, for example, in Fig. 6 for a loop of 37 SIAs. Loops of rhombus shape, with sides along ⟨1 1 2⟩ directions, are slightly more stable and, when having more than 64 SIAs, dissociate on their glide prism into Shockley partial dislocations separated by a

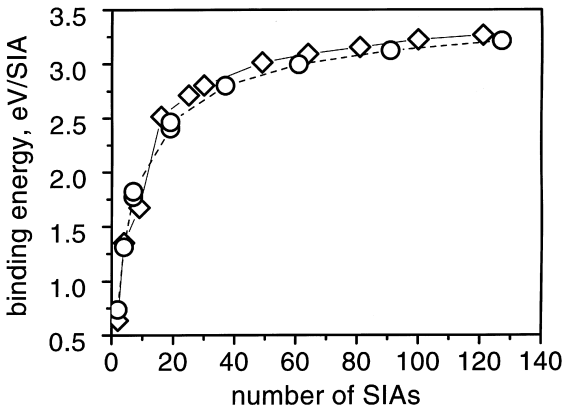


Fig. 4. Binding energy for different SIA loops in Cu modelled using the LRPP. Circle: sets of ⟨1 0 0⟩ dumbbells and (1/3) ⟨1 1 1⟩ {1 1 1} Frank loops. Square: sets of ⟨1 1 0⟩ crowdions and (1/2) ⟨1 1 0⟩ {1 1 0} perfects loops.

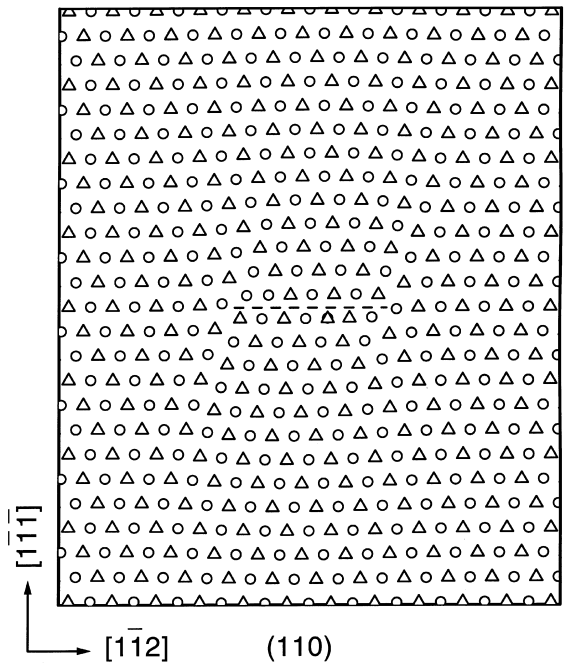


Fig. 5. (1 1 0) cross-section of the hexagonal Frank loop with $N_I = 37$ in Cu modelled using the LRPP. The dashed line indicates the trace of the stacking fault.

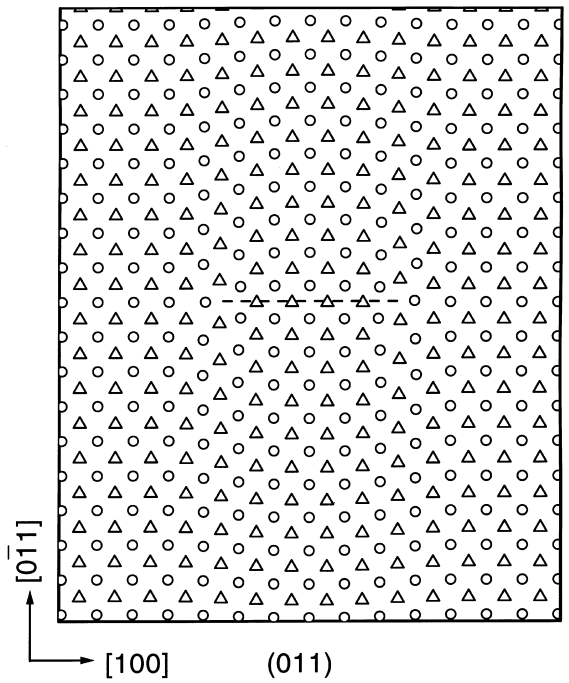


Fig. 6. (1 1 0) cross-section of the hexagonal (1/2) ⟨1 1 0⟩ {1 1 0} loop with $N_I = 37$ in Cu modelled using the LRPP. The dashed line indicates the trace of the loop habit plane.

ribbon of intrinsic stacking fault. These features can be seen in Fig. 7 where the $(\bar{1}\,1\,1)$ cross-section through a loop with 121 SIAs is presented.

Therefore, unlike the case of Fe, two types of stable clusters are formed in Cu: glissile clusters of $\langle 1\,1\,0\rangle$ crowdions forming perfect (1/2) $\langle 1\,1\,0\rangle$ loops and sessile clusters of $\langle 1\,0\,0\rangle$ dumbbells forming faulted Frank loops (1/3) $\langle 1\,1\,1\rangle$.

### 2.3. Vacancy clusters and loops in iron

Compact vacancy clusters and loops have been studied using both types of potentials [11,27,39–41]. In general, the stability is low relative to that of interstitial clusters. Two types of vacancy clusters are found to be most stable, namely a set of di-vacancies in the second coordination sphere concentrated in two adjacent $\{1\,0\,0\}$ planes and a compact set of first neighbour vacancies in a $\{1\,1\,0\}$ plane. During growth the first type results in a perfect dislocation loop with Burgers vector $\langle 1\,0\,0\rangle$ whereas the second unfaults into a (1/2) $\langle 1\,1\,1\rangle$ perfect loop. Unlike interstitial clusters and loops, vacancy loops can be stable in a static lattice in the faulted (1/2) $\langle 1\,1\,0\rangle$ configuration. Depending on the potential, these loops can unfault when having more than 40–60 vacancies. The unfaulting process is found to depend on the local conditions. Thus isolated loops unfault into (1/2) $\langle 1\,1\,1\rangle$ perfect ones whereas (1/2) $\langle 1\,1\,0\rangle$ loops having defects around them can unfault into $\langle 1\,0\,0\rangle$ perfect loops [40].

Note that both types of perfect loop are intrinsically glissile. The stability of perfect loops increases with size and those having $> 40$ vacancies are stable at all temperatures. A comparison of the binding energy versus size for different loops obtained with the LRPP is presented in Fig. 8. It can be seen that whereas small clusters of $\langle 1\,0\,0\rangle$ type are slightly more stable, the situation is reversed for bigger clusters and loops. We do not present the structure of vacancy loops because it is similar to those of SIA loops [23] and some examples can be found elsewhere [27,39].

Comparison of results for the LRPP and the MBP shows that the main difference is in the unfaulting process [27]. Thus faulted clusters do not unfault during relaxation using a MBP although large loops (>40–50 vacancies) are more stable in the perfect form. This reflects another qualitative difference between the potentials, in that the short-range, many-body equilibrium potentials usually produce three-dimensional, compact vacancy clusters (microvoids) as the most stable configuration (see also [11]).

### 2.4. Vacancy clusters in copper

Results of numerous studies of vacancy clusters in Cu [22,34,42–44] with long-range pair potentials have shown that the most stable configurations are stacking fault tetrahedra (SFT) and faulted clusters on $\{1\,1\,1\}$ planes, the latter resulting in faulted Frank loops (1/3) $\langle 1\,1\,1\rangle$ $\{1\,1\,1\}$. Examples of atomic structures can be found in [22,31,42,43]. These results are consistent with experiment and explain the features of the size distribution of SFT formed under different conditions

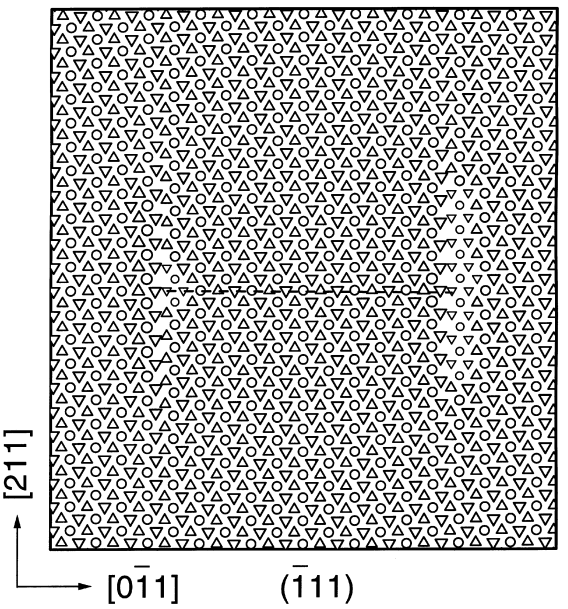


Fig. 7. $(\bar{1}\,1\,1)$ cross-section through the centre of rhombus loop with $N_I = 121$ in Cu after dissociation. The horizontal dashed line indicates the trace of habit plane of the loop before dissociation.

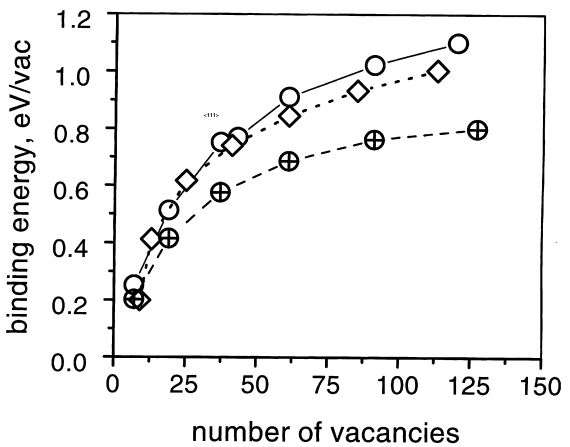


Fig. 8. Binding energy of vacancy loops in Fe calculated with the LRPP: open circles: (1/2) $\langle 1\,1\,1\rangle$ perfect loops; diamonds: $\langle 1\,0\,0\rangle$ perfect loops; crossed circles: (1/2) $\langle 1\,1\,0\rangle$ faulted loops.

[45–47]. The binding energy versus size for different clusters and loops is presented in Fig. 9. It should be noted that although (1/2) ⟨1 1 0⟩ {1 1 0} perfect vacancy loops have high binding energy, at non-zero temperature they dissociate into SFT-like sessile configurations [27]. Therefore all stable vacancy clusters in Cu are intrinsically sessile.

The properties of vacancy clusters simulated with different potentials are compared in [22,34]. In general, vacancy clusters simulated with a MBP do not collapse into dislocation loops or SFT during static relaxation. As in Fe, this reflects the fact that small, three-dimensional vacancy clusters are more stable with MBPs. For large enough size, if a cluster is induced to collapse, e.g. due to previous relaxation with the LRPP, it can be stable with the MBP [22,34].

## 3. Mobility of defect clusters and dislocation loops

### 3.1. Small interstitial clusters

The mobility of small interstitial clusters ($N_I \leqslant 19$) in Fe and Cu has been studied intensively in recent years [10,11,24–28,35] and the following conclusions can be drawn. First, di- and tri-interstitials in both Fe and Cu exhibit a combination of one-dimensional fast glide along the crowdion direction and occasional rotation to an equivalent direction. The frequency of rotation is lower for tri-interstitials and increases at high temperature for both defects. In effect, this motion is three-dimensional. Some diffusional characteristics of small clusters have been obtained by analysis of mean square displacements and jump frequencies. Thus, the three-dimensional diffusion coefficient of a di-interstitial in Cu was obtained in [24,25] and the activation energy was estimated to be about 0.046 eV. Analysis of jumps and rotation yielded a migration energy of 0.037 eV for ⟨1 1 0⟩ glide, 0.083 eV for the ⟨1 0 0⟩ dumbbell mechanism and 0.103 eV for rotation. In [11] both di- and tri-interstitials in Fe were treated by three-dimensional diffusion and the activation energy was found to decrease from 0.083 eV for 2-SIAs to 0.061 eV for 3-SIAs, compared with 0.167 eV for a single interstitial.

MD simulations of larger clusters of crowdions (from 4 to 19 SIAs) in both Fe and Cu show that motion is due solely to one-dimensional glide along the corresponding crowdion direction [23–25,32,33].

### 3.2. Interstitial dislocation loops

The mobility of interstitial dislocation loops, i.e., clusters containing more than about 20–30 interstitials, in Fe and in Cu has been studied in [29,28] for $N_I$ up to 100. Unlike the situation for small clusters, the results for Fe and Cu are qualitatively different.

In Fe all loops exhibit the same thermally activated, one-dimensional motion as smaller clusters (see Section 3.1). During simulation these loops produce significant atomic displacements only along one direction, namely that of ***b***, as demonstrated in Fig. 10(a) for a loop of 37 SIAs at 260 K. Analysis of the atomic displacements

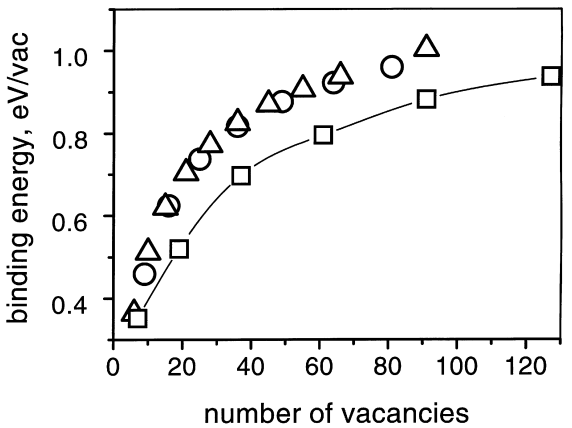


Fig. 9. Binding energy of vacancy clusters and loops in Cu calculated with the LRPP: circles: (1/2) ⟨1 1 0⟩ perfect loops, triangles – stacking fault tetrahedra, squares: (1/3) ⟨1 1 1⟩ faulted Frank loops.

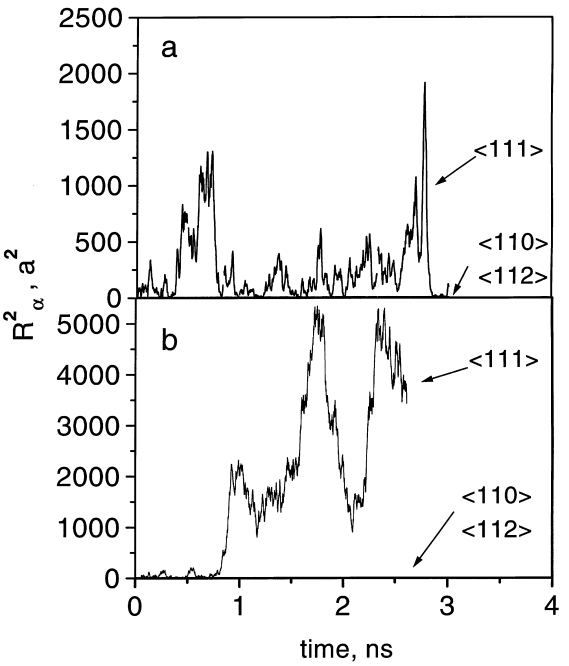


Fig. 10. Sum of the square of atomic displacements projected onto three orthogonal directions during thermal annealing of a model crystal of α-Fe containing: (a) a (1/2) ⟨1 1 1⟩ 37-SIA loop at 260 K and (b) a (1/2) ⟨1 0 0⟩ 37-VAC loop at 300 K.

produced during annealing shows that only atoms inside the glide prism are displaced, as demonstrated in Fig. 11(a) by the set of instantaneous positions of atoms in the cross-section of the crystallite containing the loop in Fig. 10(a). The positions were recorded every 10 ps over a time of 400–600 ps.

The jumps of individual ⟨1 1 0⟩ crowdions in a cluster in Cu can be distinguished only for loops having $\leqslant 25$ SIAs. Bigger loops (up to 64–81 SIAs) move one-dimensionally but their motion is impossible to decompose into discrete jumps of their individual crowdions, due to the fact that such loops dissociate on their glide prism (see Section 2.1) and cannot be described as sets of individual crowdions. MD simulation shows that loops from 49 to 81 SIAs can periodically dissociate and associate during annealing. They are mobile in the latter state but immobile in the former. The proportion of the time when a loop is in the dissociated state decreases with temperature and increases with loop size. The biggest loop studied ($N_I = 100$) was found to be practically immobile in the temperature range 240–860 K [27].

### 3.3. Vacancy dislocation loops

It has been found very recently that perfect vacancy loops in Fe are mobile [27,28]. A full study is in progress and adequate statistics for jumps are available only for (1/2) ⟨1 1 1⟩ loops of 37 and 43 vacancies. MD simulations over a wide temperature range have shown that such loops can migrate by thermal activation in one-dimension, similar to the interstitial loops described above. To demonstrate the similarity we present in Fig. 10(b) the time dependence of the sum of the square of atomic displacements along the direction of $\boldsymbol{b}$ and two orthogonal directions obtained for a loop containing 37

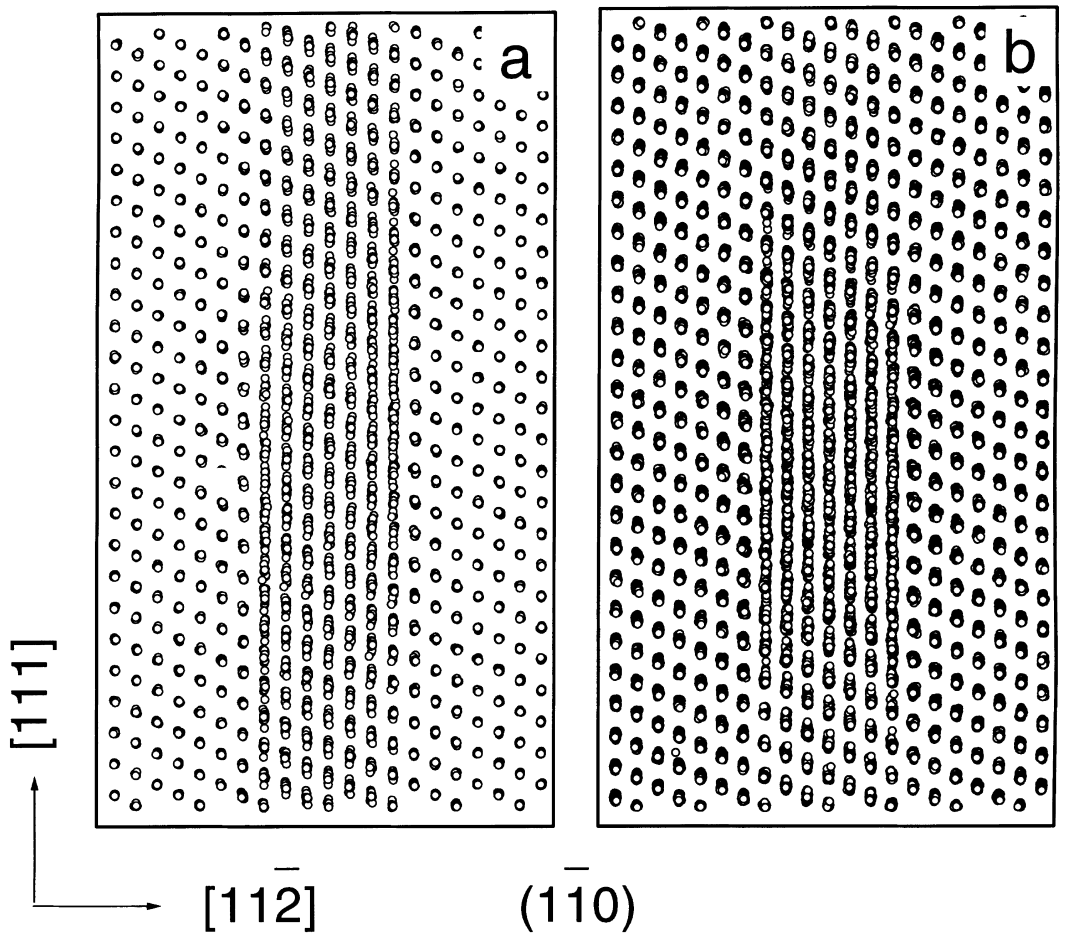


Fig. 11. (1 $\bar{1}$ 0) projection of atoms in a cross-section of a crystallite of Fe containing: (a) a (1/2) ⟨1 1 1⟩ 37-SIA loop at 260 K and (b) a (1/2) ⟨1 1 1⟩ 37-VAC loop at 300 K. The positions of the atoms were recorded every 10 ps for 400 ps (SIA loop) and 600 ps (VAC loop) and are superimposed in these plots.

vacancies during annealing at 300 K. The behaviour is qualitatively similar to that for a SIA loop of the same size (Fig. 10(a)). Another similarity can be found by comparing superimposed atomic projection of the interstitial and vacancy loops in Fig. 11(a) and (b), respectively. It can be seen that both types of loop behave similarly and only atoms inside the glide prism are displaced during loop motion.

### 3.4. Parameterisation of cluster motion

The parameters of cluster mobility within the diffusional approximation have been determined by analysing both the mean square displacements (MSD) produced by atoms and the jump frequency of the centre of mass (CM) of gliding loops [24–28]. The self-diffusion coefficient in a crystallite containing a cluster can be obtained from the MSD whereas the diffusivity of a cluster can be estimated from the jump frequency analysis. Treatment of MSD using the method suggested in [48] and successfully applied there and in [24–27] for three-dimensional diffusion of the mono-interstitial in W, Fe and Cu and for the di-interstitial in Cu, gives unsatisfactory results for larger clusters due to a high statistical error in estimating the diffusion coefficient. The typical error is about 25–45% and leads to a large uncertainty in the activation energy, which can even be estimated as negative [23–25]. Better results are obtained by the analysis of the displacements of the CM of clusters, defining a cluster jump to occur when the CM is displaced by $\boldsymbol{b}$. Reasonable statistics have been obtained from 700 to 1100 jumps at different temperatures for clusters and loops containing up to 91 SIAs, for this allows the jump frequency to be estimated with a statistical accuracy of 2–4%. Jump frequency $\nu^n$ for a cluster of $n$ SIAs versus reciprocal temperature for some clusters in Fe and Cu is presented in Fig. 12. All plots in these figures are close to linear and therefore the Arrhenius-like relationship has been applied to describe the one-dimensional diffusional transport behaviour of the clusters:

$$\nu^n = \nu_0^n \exp\left(-\frac{E_n^m}{k_B T}\right), \tag{1}$$

where $\nu_0^n$ is the pre-exponential factor of the cluster, $k_B$ the Boltzmann constant and $E_n^m$ is the 'effective' activation energy for jumps of the cluster. The results of this treatment are presented in Tables 1 and 2 for all one-dimensionally mobile SIA clusters studied in Fe and Cu, together with the results for the low-temperature $\langle 1\,1\,1\rangle$ crowdion mechanism for the single-interstitial in Fe and the $\langle 1\,1\,0\rangle$ crowdion mechanism for the di-interstitials in Cu [23–28,40]. It can be seen that for both Fe and Cu the activation energy is weakly dependent on the size of cluster. This allows Eq. (1) to be generalised to find a simple size dependence of cluster jump frequency

$$\nu^n = \nu_0 n^{-S} \exp\left(\frac{-\langle E^m\rangle}{k_B T}\right), \tag{2}$$

where $\langle E^m\rangle$ is the averaged effective activation energy and $\nu_0$ is a new, size-independent, pre-exponential factor. The value of $\langle E^m\rangle$ is estimated from the tables as $0.023 \pm 0.003$ eV for (1/2) $\langle 1\,1\,1\rangle$ clusters in Fe and $0.024 \pm 0.003$ eV for (1/2) $\langle 1\,1\,0\rangle$ clusters in Cu. Using these energies, the parameters $\nu_0$ and $S$ were obtained by fitting to the pre-exponential factors presented in Tables 1 and 2. The values $\nu_0 = 6.1 \times 10^{12}$ s$^{-1}$, $S = 0.66$ for Fe

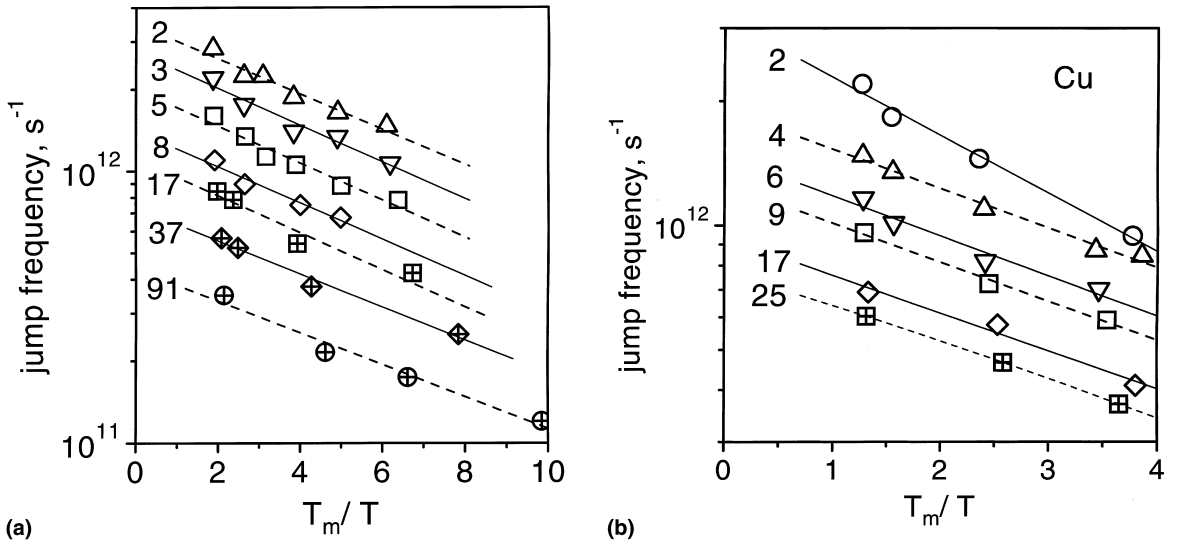


Fig. 12. Jump frequency versus reciprocal temperature for different SIA clusters in (a) Fe and (b) Cu.

Table 1
Results of the treatment of the jump frequency for stable clusters in Fe using an Arrhenius-like dependence[a]

| Type, $N_D$ | $v_0$ [$10^{12}$ $s^{-1}$] | $E^m$ (eV) |
|---|---|---|
| SIA clusters | | |
| ⟨1 1 1,⟩, 1 | 6.36 | 0.023 ± 0.003 |
| ⟨1 1 1,⟩, 2 | 3.49 | 0.023 ± 0.003 |
| ⟨1 1 1,⟩, 3 | 2.76 | 0.024 ± 0.003 |
| ⟨1 1 1,⟩, 5 | 2.01 | 0.024 ± 0.003 |
| ⟨1 1 1,⟩, 8 | 1.41 | 0.025 ± 0.006 |
| ⟨1 1 1,⟩, 17 | 1.11 | 0.025 ± 0.006 |
| ⟨1 1 1,⟩, 19 | 1.07 | 0.023 ± 0.004 |
| ⟨1 1 1,⟩, 28 | 0.87 | 0.021 ± 0.003 |
| ⟨1 1 1,⟩, 37 | 0.73 | 0.022 ± 0.003 |
| ⟨1 1 1,⟩, 91 | 0.44 | 0.021 ± 0.004 |
| ⟨1 1 1,⟩, 16 | 0.31 | 0.028 ± 0.003 |
| VAC clusters | | |
| ⟨1 1 1,⟩, 37 | 0.33 | 0.011 ± 0.004 |
| ⟨1 1 1,⟩, 43 | 0.31 | 0.010 ± 0.004 |

[a] $N_D$ is the number of SIAs or vacancies, $E^m$ is the effective migration energy and $v_0$ is the jump frequency pre-exponential factor. The simulations were carried out using the LRPP.

Table 2
Results of the treatment of the jump frequency for SIA clusters in Cu using an Arrhenius-like dependence (the simulations were carried out using the LRPP)

| Type, $N_D$ | $v_0$ [$10^{12}$ $s^{-1}$] | $E^m$ (eV) |
|---|---|---|
| SIA clusters | | |
| ⟨1 1 0,⟩, 2 | 3.16 | 0.038 ± 0.003 |
| ⟨1 1 0,⟩, 4 | 1.91 | 0.026 ± 0.003 |
| ⟨1 1 0,⟩, 6 | 1.47 | 0.026 ± 0.004 |
| ⟨1 1 0,⟩, 9 | 1.24 | 0.025 ± 0.002 |
| ⟨1 1 0,⟩, 17 | 0.89 | 0.021 ± 0.002 |
| ⟨1 1 0,⟩, 25 | 0.74 | 0.020 ± 0.002 |

and $v_0 = 4.7 \times 10^{12}$ $s^{-1}$, $S = 0.61$ for Cu describe the MD data very well, as can be seen in Fig. 13.

The diffusion-like treatment should also include the analysis of correlations in cluster motion. This has been done in [25] by treating the statistics of forward and backward jumps for different clusters in Fe and Cu. In general, all clusters and loops have a preference for jumps in the same direction as their previous jump, which means that the correlation factor is larger than unity and their motion is not described as one-dimensional random walk. However this interpretation depends on the definition of cluster step length in diffusional motion. Thus, it is possible to obtain a value of correlation factor equal to unity by increasing the length of jump. In this case, the effective jump length is a temperature-dependent parameter which increases at low temperature. In [25] a constant jump vector (equal to the Burgers vector corresponding to the particular type of cluster) was used which allows a formal application of an Arrhenius-type treatment of cluster jump

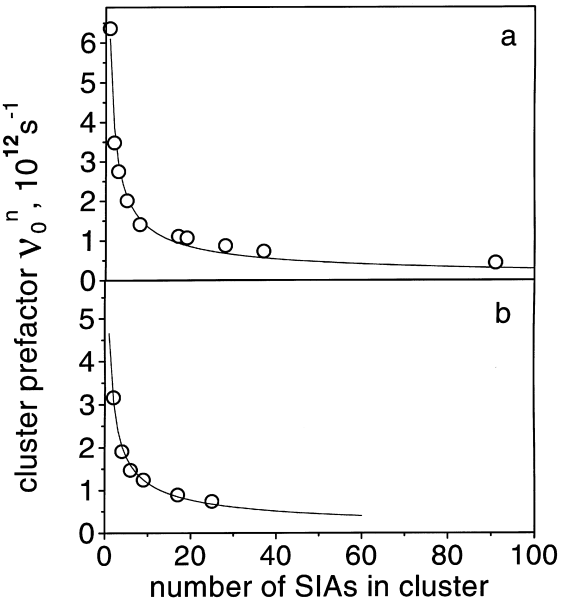


Fig. 13. Size dependence of pre-exponential factor in the Arrhenius-like treatment of the jump frequency in (a) Fe and (b) Cu.

frequency. For a given definition of cluster step length, the value of the correlation factor depends on the cluster type and size and the temperature. The temperature-dependence of the correlation factor for some SIA clusters in Fe and Cu is presented in Fig. 14. It can be seen that the value of the correlation factor increases at low temperature and decreases for larger clusters. The nature of the effect has been discussed in [25]. A special study has been carried out in order to prove that this is not an artefact of the simulation model by studying the jump frequency and correlation factor of a cluster of 19 SIAs in Fe crystallites of different sizes with periodic boundary conditions. The crystallite size was varied from $10a$ to $100a$, where $a$ is the lattice parameter in the glide direction. It was found that the cluster is unstable and can change its glide direction in the smallest crystallite due to the interaction with its images, but in crystallites bigger than $15a$ the cluster is stable and performs one-dimensional glide. The jump frequency increases slightly with crystallite size and saturates at about 50–60$a$, whereas the value of the correlation factor is only weakly size-dependent (see Fig. 15). It was concluded in [25] that a value bigger than 1 for the correlation factor is an intrinsic property of gliding clusters.

The one-dimensional motion of vacancy clusters can also be treated by the Arrhenius-like relationship for the jump frequency of the CM and the results obtained in [27] for 37- and 43-vacancy loops in Fe are presented in Fig. 16 and Table 1. It can be seen that $E_m$ and $v_0$ are

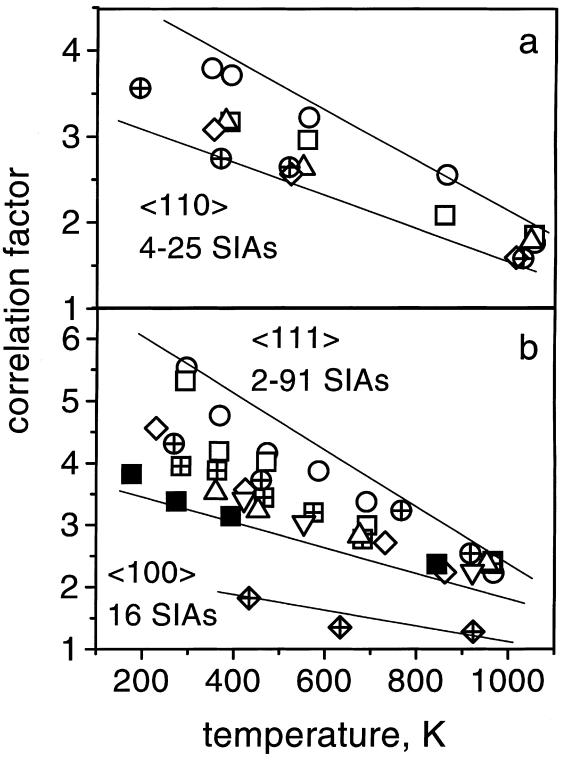


Fig. 14. Temperature dependence of the correlation factor for one-dimensional jumps of different SIA clusters of (a) size ranging from $N_I = 4$ (open circles) to $N_I = 25$ (crossed circles) in Cu and (b) size ranging from $N_I = 2$ (open circles) to $N_I = 91$ (full squares) in Fe. A LRPP was used in both models.

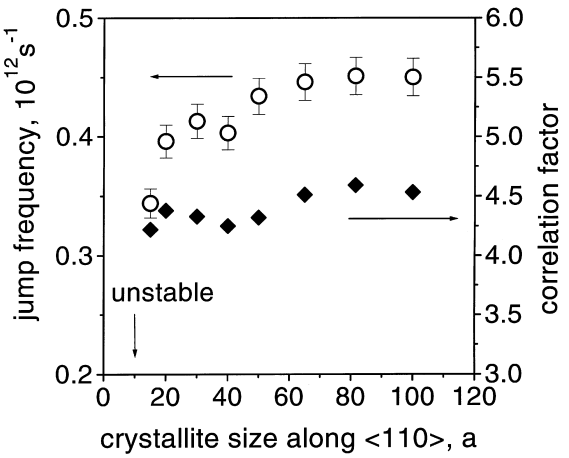


Fig. 15. Dependence of jump frequency (circles) and correlation factor (full diamonds) for 19-SIAs cluster in Fe versus crystallite size.

about half of the value of the same parameters for a SIA loop of the same size. The correlation factor for vacancy loop jumps is qualitatively similar to that for SIA loops

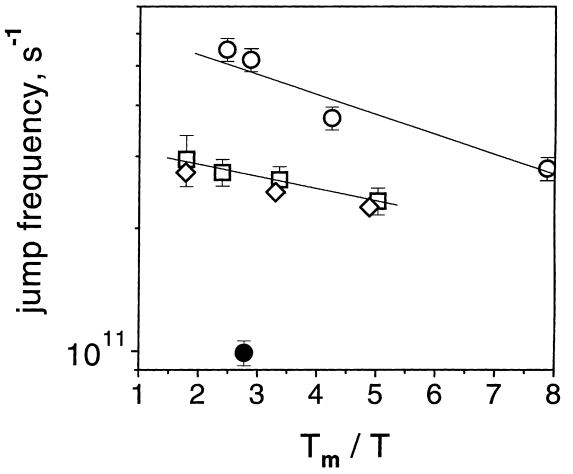


Fig. 16. Jump frequency versus reciprocal temperature for some vacancy and SIA loops in Fe. Circles: 37-SIA; squares: 37-VAC; diamonds: 47-VAC (all calculated with the LRPP). Filled circle is a 61-VAC loop at 652 K with the MBP.

but with a slightly lower value. It should be noted that these results were obtained for the LRPP. The thermal stability of perfect vacancy loops simulated with the MBP is lower, but a hexagonal loop of 61 vacancies is stable and exhibits a similar mobility: its jump frequency at 652 K is also presented in Fig. 16.

### 3.5. Mechanisms of one-dimensional motion of clusters and loops

Although the treatment of SIA cluster motion results in an Arrhenius-like dependence of cluster jump frequency on temperature, it is not certain that one-dimensional motion of clusters can be described formally as conventional diffusion. The main arguments are the extremely low activation energy and the non-random character of jumps. In most simulations the thermal energy per atom is higher than the estimated activation energy and therefore this process cannot be described as a thermally activated jump over a specific barrier. On the other hand, all clusters studied have a linear dependence of jump frequency on reciprocal temperature, and in the case of Fe the value of the activation energy is very similar to the migration energy of a single SIA via the low-temperature $\langle 1\,1\,1\rangle$ crowdion mechanism. This result is considered to be important because it links the mechanism of mobility with the activation energy. In fact it has been seen that the motion of small SIA clusters and loops is the result of the motion of individual crowdions [8,23–25,35,49,50], so that it is perhaps not surprising that the activation energy of cluster motion is the same as that for a single crowdion. However, the pre-exponential factor $\nu_0^n$ is size-depen-

dent, reflecting the size-dependence of the probability of moving all the crowdions in the same direction. It is interesting to note that the size-independent pre-exponential factor $v_0$ fitted for SIA clusters in Fe is very similar to the pre-exponential factor of jump frequency of low-temperature diffusion of a single crowdion obtained for the same potential [23–25]. We believe this coincidence also confirms that it is physically feasible to link the properties of the single crowdion with those of an SIA cluster (e.g., presented in Eq. (2)). Unfortunately, a similar correlation cannot be found for Cu because a single SIA does not migrate via the $\langle 1\,1\,0\rangle$ crowdion mechanism in that metal [23–25].

Another aspect of cluster motion was studied in [50]. A special MD study was performed using the MBP for 3, 9 and 17-SIAs clusters in Fe. Jump frequencies for both the centre of mass of a cluster and each individual crowdion were obtained. Different stochastic models were tested using Monte Carlo simulation and it was found that the model of weakly coupled particles, i.e., crowdions in this case, gives a good description of the MD results. It was found that the jump frequency of the crowdions in a cluster is an increasing function of cluster size. This is believed to be due to enhanced focusing of the crowdion configuration for SIAs in a cluster, which results in increasing probability of their successive jumps. A similar effect, i.e., stronger focusing of the crowdion configuration of SIAs in a cluster with decreasing temperature, is proposed to be responsible for the deviation of cluster jump frequency from the Arrhenius relationship which occurs at low temperatures.

The above features of SIA cluster mobility in one-dimension should be related to the time-scale of molecular dynamics simulation i.e., $\approx 10^{-9}$ s. The estimated mean free path and the lifetime of these clusters are rather large ($\approx$1–10 μm and $\approx 10^{-3}$ s [12,13]) and MD simulation cannot predict the behaviour at this scale. Nevertheless, the results discussed here show that the probability to change direction of glide (cluster rotation) decreases for large clusters and the character of SIA cluster mobility should be accepted at least as 'preferentially one-dimensional' (for definition see e.g., [51]).

## 4. Similarities and differences in properties of defect clusters in Fe and Cu

The results of atomistic simulation studies described above illustrate a number of similarities and differences in properties of defect clusters in Fe and Cu. The biggest difference is observed in mobility properties of stable cluster and loops.

Thus, vacancy clusters in Cu simulated with different long-range pair potentials have a high stability when in the form of stacking fault tetrahedra. High stability means not only a high binding energy, which depends on the potential, but also stability when simulated by molecular dynamics at non-zero temperature. Thus SFTs are stable at least up to 920 K [22]. The stability of Frank loops depends on the shape, size and temperature. For example, an hexagonal loop containing 37 vacancies becomes unstable at 920 K after a few hundred ps. High binding energy but low configurational stability have also been observed for perfect (1/2) $\langle 1\,1\,0\rangle$ loops. All unstable vacancy clusters and loops in Cu transform into SFT-like configurations. Therefore, all stable vacancy clusters and loops in Cu are sessile.

Vacancy clusters in Fe can have a rather high binding energy (e.g., see Fig. 3) but a rather low stability. Thus all clusters and loops containing up to 37 vacancies are unstable and transform into a flexible three-dimensional sets of second-neighbour vacancies. Although these clusters are highly mobile, in comparison with the mono-vacancy [52], their mobility is three-dimensional and much lower than that of mono-interstitials and SIA clusters migrating one-dimensionally. During further growth under high vacancy supersaturation conditions such clusters can transform into perfect loops with Burgers vectors (1/2) $\langle 1\,1\,1\rangle$ and $\langle 1\,0\,0\rangle$ [40,41]. Unlike stable vacancy clusters in Cu, these loops in Fe are intrinsically glissile and exhibit one-dimensional thermally activated motion [28].

The qualitative difference is found in properties of interstitial clusters and loops in Cu and Fe. Thus, two types of stable SIA loop exist in Cu, namely sessile faulted Frank loop (1/3) $\langle 1\,1\,1\rangle$ and glissile perfect loop (1/2) $\langle 1\,1\,0\rangle$ whereas only glissile perfect loops (1/2) $\langle 1\,1\,1\rangle$ and $\langle 1\,0\,0\rangle$ are stable in Fe.

Glissile SIA clusters and loops in both metals show similar properties i.e. three-dimensional motion of small clusters (less than 4 SIAs) and fast thermally-activated one-dimensional motion of bigger clusters. A difference appears only for big loops due to the dissociation of (1/2) $\langle 1\,1\,0\rangle$ perfect loops in Cu, for loops having more that 100 SIAs become immobile. In contrast, there is no mechanism for preventing thermally activated one-dimensional transport of isolated SIA loops in Fe.

## 5. Implications for damage accumulation

Having identified the difference in the intrinsic properties of clusters and loops in Section 4, it is of interest to examine the relevance and implications of these differences for the problem of defect accumulation under cascade damage conditions. As indicated already in Section 1, a detailed understanding of the properties of clusters produced in cascades is necessary to rationalize the observed differences in the defect accumulation behaviour between bcc and fcc metals [19]. The experimental results shown in Fig. 1 provide a more

recent example of the difference in the defect accumulation behaviour between bcc iron and fcc copper [20].

Two important differences in the properties of clusters and loops have been emerged from the recent works:

1. All stable SIA clusters and loops in Fe are glissile and perform thermally-activated motion in one-dimension, whereas only a fraction of SIA clusters and loops in copper is expected to be glissile;
2. All stable vacancy clusters and loops in Cu are intrinsically sessile, whereas those in Fe are likely to perform one-dimensional transport by thermally activated motion.

It is interesting to note here that these differences are similar to the factors that Singh and Evans [19] found necessary to explain the lower density of clusters in bcc metals compared to that in fcc metals. The fact that all stable clusters and loops in iron are glissile means that the accumulation of clusters will be determined by the reaction kinetics of one-dimensionally gliding clusters in the three-dimensional lattice. In addition, a substantial fraction of the gliding clusters will be lost to sinks such as dislocations, grain boundaries, etc. Furthermore, the annihilation interactions between gliding SIA and vacancy clusters in Fe would cause a further loss of clusters [26]. All these factors would lead to a lower cluster density in iron. In the case of copper, on the other hand, the continuous production of sessile clusters of SIAs and vacancies in the cascades would ensure the accumulation of a high density of clusters. Thus, the difference in the properties of clusters discussed in Section 4 provides at least a qualitative explanation for the observed differences in clusters density between iron and copper (Fig. 1). Similar argument can be used to understand the lower cluster density in Mo than that in copper [19].

It is also of interest to note that most of the vacancy loops and large interstitial loops in copper dissociate and lose their ability to glide by a thermally-activated process. It seems reasonable to assume that this dissociation occurs due to the low stacking fault energy (SFE) of 35–42 mJ/m$^2$ [53], which is reproduced with the potentials used in the simulations discussed here. This implies that in fcc metals with high stacking fault energy, a fraction of loops which may not dissociate and would thereby remain mobile. In other words, in metals such as Ni and Al with a SFE of 120–130 mJ/m$^2$ [54] and 154 mJ/m$^2$ [55], respectively, the fraction of mobile clusters and loops would be higher than Cu. Consequently, for a given set of irradiation conditions, the cluster density should be highest in Cu and lowest in Al. Cluster densities measured by TEM in neutron irradiated Cu, Ni and Al at $0.33T_m$, where $T_m$ is the melting temperature, to a dose level of $\approx$0.1 dpa have been reported to be $\approx 1\times10^{24}$, $\approx 5\times10^{21}$ and $\approx 1\times10^{20}$ m$^{-3}$, respectively [56]. At an irradiation temperature of 0.42 $T_m$ and dose level of $\approx$0.1 dpa, the cluster density in copper has been reported to be $\approx 1\times10^{22}$ m$^{-3}$ compared to only $\approx 2\times10^{19}$ m$^{-3}$ in Al [57]. These results may be taken to suggest that stacking fault energy may play a significant role in determining the magnitude of defect accumulation in the form of clusters and loops.

The influence of these differences in the properties of clusters and loops in the accumulation of voids in bcc and fcc metals has been treated within the framework of the production bias model in a separate paper [18] and will not be discussed here.

## 6. Conclusions

1. Data on the structure and properties of defect clusters and dislocation loops in Fe and Cu obtained recently by atomic-scale computer simulation have been described and discussed.
2. The most stable interstitial clusters and dislocation loops in α-Fe are glissile sets of $\langle 1\,1\,1\rangle$ or $\langle 1\,0\,0\rangle$ crowdions. These clusters and loops perform a thermally activated, one-dimensional motion in the crowdion direction.
3. Stable vacancy clusters in Fe are glissile $(1/2)\langle 1\,1\,1\rangle$ and $\langle 1\,0\,0\rangle$ dislocation loops.
4. Stable interstitial clusters and dislocation loops in Cu can be either glissile ($\boldsymbol{b} = (1/2)\ \langle 1\,1\,0\rangle$) or sessile ($\boldsymbol{b} = (1/3)\ \langle 1\,1\,1\rangle$). Small glissile clusters (up to 49 SIAs) perform thermally activated, one-dimensional motion along $\langle 1\,1\,0\rangle$ directions. Large glissile loops (more than 81–100 SIAs) are immobile due to the dissociation of the dislocation on the glide prism.
5. At zero temperature stable vacancy clusters in Cu are either glissile $(1/2)\ \langle 1\,1\,0\rangle$ and sessile $(1/3)\ \langle 1\,1\,1\rangle$ loops or sessile stacking fault tetrahedra. During annealing glissile vacancy loops dissociate into sessile SFT-like configurations
6. Two parameters, stacking fault energy and size, control stability and mobility of defect clusters in fcc metals.
7. It remains uncertain whether or not the one-dimensional thermally activated motion of glissile clusters and dislocation loops can be described as a conventional diffusion process although it obeys an Arrhenius-like dependence for jump frequency.

## Acknowledgements

We are grateful to Dr A.V. Barashev and Dr F. Gao for numerous discussions. This research has been carried out using the facilities of CESCA and CEPBA (Barcelona, Spain) under the coordination of C4. The authors also acknowledge financial support from the University of Liverpool (Yu.N.O) and the UK Engineering and Physical Sciences Research Council also.

## References


[1] D.J. Bacon, T. Diaz de la Rubia, J. Nucl. Mater. 216 (1994) 275.
[2] T. Diaz de la Rubia, Ann. Rev. Mater. Sci. 26 (1996) 213.
[3] D.J. Bacon, A.F. Calder, F. Gao, J. Nucl. Mater. 251 (1997) 1.
[4] D.J. Bacon, F. Gao, Yu.N. Osetsky, Proc. COSIRES-98, Nucl. Instrum. and Meth. B 153 (1999) 87.
[5] D.J. Bacon, F. Gao, Yu.N. Osetsky, these Proceedings, p. 1.
[6] T. Diaz de la Rubia, M. Guinan, Mater. Sci. Forum 97&98, (1992) 23.
[7] A.J.E. Foreman, C.A. English, W.J. Phythian, Philos. Mag. A 66 (1992) 655.
[8] A.F. Calder, D.J. Bacon, J. Nucl. Mater. 207 (1993) 25.
[9] W.J. Phythian, R.E. Stoller, A.J.E. Foreman, A.F. Calder, D.J. Bacon, J. Nucl. Mater. 223 (1995) 245.
[10] R. Stoller, G.R. Odette, B.D. Wirth, J. Nucl. Mater. 251 (1997) 49.
[11] N. Soneda, T. Diaz de la Rubia, Philos. Mag. 78 (1998) 995.
[12] H. Trinkaus, B.N. Singh, A.J.E. Foreman, J. Nucl. Mater. 199 (1992) 1.
[13] H. Trinkaus, B.N. Singh, A.J.E. Foreman, J. Nucl. Mater. 206 (1993) 200.
[14] C.H. Woo, B.N. Singh, Phys. Stat. Sol. (b) 159 (1990) 609.
[15] C.H. Woo, B.N. Singh, Philos. Mag. A 65 (1992) 889.
[16] B.N. Singh, A.J.E. Foreman, Philos. Mag. A 66 (1992) 975.
[17] B.N. Singh, S.I. Golubov, H. Trinkaus, A. Serra, Yu.N. Osetsky, A.V. Barashev, J. Nucl. Mater. 251 (1997) 107.
[18] S.I. Golubov, B.N. Singh, H. Trinkaus, these Proceedings, p. 78.
[19] B.N. Singh, J.H. Evans, J. Nucl. Mater. 226 (1995) 277.
[20] B.N. Singh, A. Horsewell, P. Toft, J. Nucl. Mater. 271&272 (1999) 97.
[21] M.L. Jenkins, M.A. Kirk, W.J. Phythian, J. Nucl. Mater. 205 (1993) 16.
[22] Yu.N. Osetsky, A. Serra, M. Victoria, V. Priego, S.I. Golubov, Philos. Mag. A, in press.
[23] Yu.N. Osetsky, A. Serra, V. Priego, B.N. Singh, S.I. Golubov, Philos. Mag. A, in press.
[24] Yu.N. Osetsky, A. Serra, V. Priego, Mater. Res. Soc. Symp. Proc. 527 (1998) 59.
[25] Yu.N. Osetsky, A. Serra, B.N. Singh, S.I. Golubov, Philos. Mag., A, unpublished.
[26] Yu.N. Osetsky, A. Serra, V. Priego, these Proceedings, p. 202.
[27] Yu.N. Osetsky, D.J. Bacon, A. Serra, Philos. Mag. Lett. 79 (1999) 273.
[28] Yu.N. Osetsky, D.J. Bacon, A. Serra, Mater. Res. Soc. Symp. Proc. 538 (1999) 649.
[29] G.J. Ackland, G. Tichy, V. Vitek, M.V. Finnis, Philos. Mag. A 56 (1987) 735.
[30] G.J. Ackland, D.J. Bacon, A.F. Calder, T. Harry, Philos. Mag. A 75 (1997) 713.
[31] Yu.N. Osetsky, A.G. Mikhin, A. Serra, Philos. Mag. A 72 (1995) 361.
[32] J.A. Moriarty, Phys. Rev. B38 (1988) 3199.
[33] J.A. Moriarty, Ibid B42 (1990) 1609.
[34] Yu.N. Osetsky, M. Victoria, A. Serra, S.I. Golubov, V. Priego, J. Nucl. Mater. 251 (1997) 34.
[35] B.D. Wirth, G.R. Odette, D. Maroudas, G.E. Lucas, J. Nucl. Mater. 244 (1997) 185.
[36] R. Bullough, R.C. Perrin, Proc. Roy. Soc. A 305 (1968) 541.
[37] J.M. Harder, D.J. Bacon, Philos. Mag. A 58 (1988) 165.
[38] R.A. Johnson, Philos. Mag. 16 (1967) 533.
[39] V.G. Kapinos, Yu.N. Osetsky, P.A. Platonov, Phys. Stat. Sol. (b) 155 (1989) 373.
[40] V.G. Kapinos, Yu.N. Osetsky, P.A. Platonov, J. Nucl. Mater. 173 (1990) 229.
[41] V.G. Kapinos, Yu.N. Osetsky, P.A. Platonov, J. Nucl. Mater. 170 (1990) 66.
[42] E.J. Savino, R.C. Perrin, J. Phys. F 4 (1974) 1889.
[43] M.J. Sabochick, S. Yip, N.Q. Lam, J. Phys. F 18 (1988) 349.
[44] V.G. Kapinos, Yu.N. Osetsky, P.A. Platonov, J. Nucl. Mater. 165 (1988) 286.
[45] A. Horsewell, B.N. Singh, S. Proennecke, W.F. Sommer, H.L. Heinisch, J. Nucl. Mater. 179–181 (1991) 924.
[46] M. Kiritani, J. Nucl. Mater. 216 (1994) 220.
[47] Y. Dai, M. Victoria, Mater. Res. Soc. Symp. Proc. 439 (1997) 319.
[48] M.W. Guinan, R.N. Stuart, R.J. Borg, Phys. Rev. B 15 (1977) 950.
[49] Yu.N. Osetsky, A. Serra, V. Priego, F. Gao, D.J. Bacon, Mater. Res. Soc. Symp. Proc. 527 (1998) 69.
[50] A.V. Barashev, Yu.N. Osetsky, D.J. Bacon, Mater. Res. Soc. Symp. Proc. 540 (1999) 697.
[51] U. Gösele, A. Seeger, J. Nucl. Mater. 34 (1976) 177.
[52] V.G. Kapinos, Yu.N. Osetsky, P.A. Platonov, J. Nucl. Mater. 184 (1991) 127.
[53] D.J. Cockayne, M.L. Jenkins, I.L.F. Ray, Philos. Mag. 24 (1971) 383.
[54] C.B. Carter, S.M. Holmes, Philos. Mag. 35 (1977) 1161.
[55] Q.H. Jin, P.J. Wang, D.T. Ding, D.S. Wang, Phys. Lett. A 174 (1993) 437.
[56] B.N. Singh, S.J. Zinkle, J. Nucl. Mater. 206 (1993) 212.
[57] A. Horsewell, B.N. Singh, in: F.A. Garner, J.S. Perrin (Eds.), Effect of Radiation on Materials, ASTM STP 870, American Society for Testing and Materisls, Philadelphia, 1985, p. 248.